A brief introduction to the *GW* method for electronic structure calculations

Min-Ye Zhang

Institute of Physics, CAS and NOMAD Laboratory at FHI of MPG

@NOMAD Coffee Talk, June 12, 2023

About me

- Born and raised in Shengze, a small town near Shanghai in Eastern China
- Studied Chemistry (BSc and PhD) at Peking University in Beijing
- Postdoctor with Professor Xinguo Ren at IOP since Nov 2021
- Visiting Berlin since Feb 2023, and will start an IOP-Humboldt fellowship from Feb 2024 ...



Name: Minye (daily use)/Min-Ye (for authorship)/Steve (used very few).

Outline

Outline

Photoemission spectroscopy

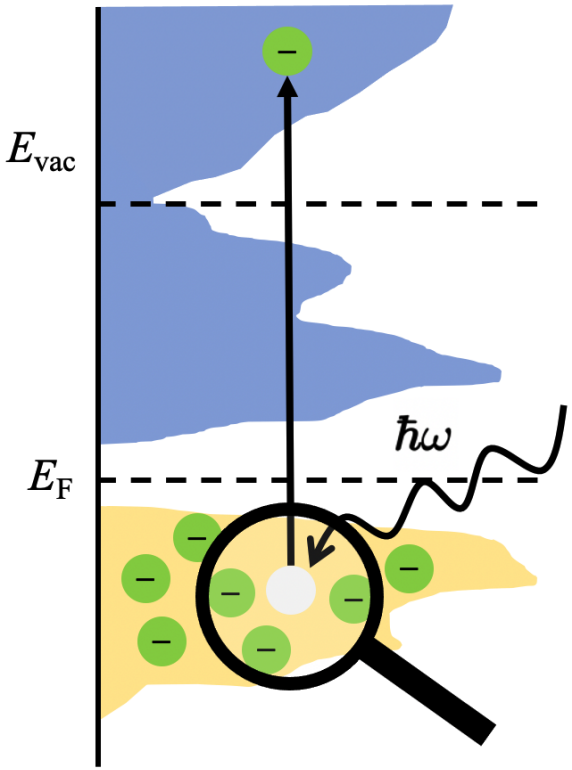

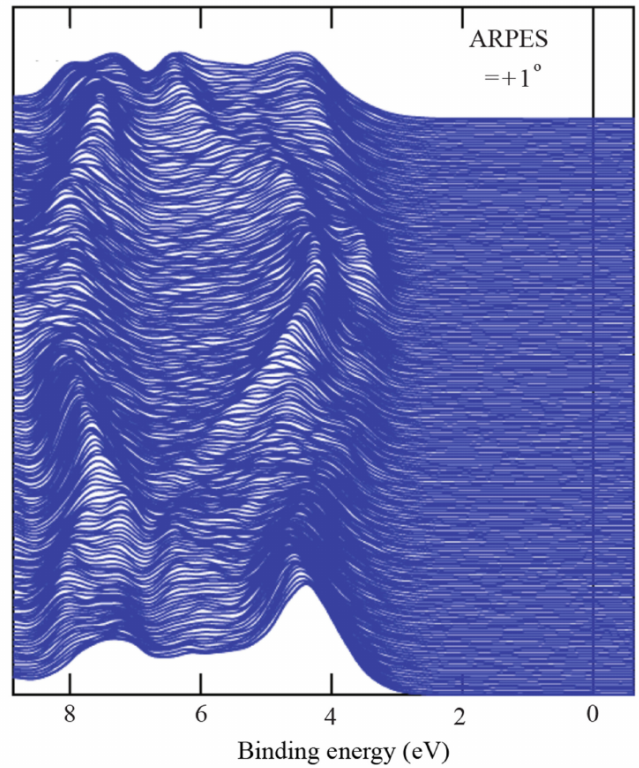

Quasiparticle: electron/hole with its surrounding as a whole, moving in a independent manner

D. Golze, M. Dvorak, and P. Rinke, Front. Chem. **7**, 377 (2019)

First-principles simulations with DFT

Kohn-Sham ansatz using certain density functional approximation (DFA)

$$\left[t_{\mathbf{r}} + v_{\text{ext}}(\mathbf{r}) + v_{\text{H}}(\mathbf{r}) + v_{\text{xc}}^{\text{DFA}}(\mathbf{r})\right]\psi_i(\mathbf{r}) = \epsilon_i^{\text{KS}}\psi_i(\mathbf{r})$$

$$v_{\text{ext}}(\mathbf{r}) = -\sum_I \frac{Z_I}{|\mathbf{r}-\mathbf{R}_I|} \qquad v_{\text{xc}}^{\text{DFA}}(\mathbf{r}) \stackrel{\text{def}}{=} \frac{\delta E_{\text{xc}}^{\text{DFA}}[n]}{\delta n(\mathbf{r})}$$

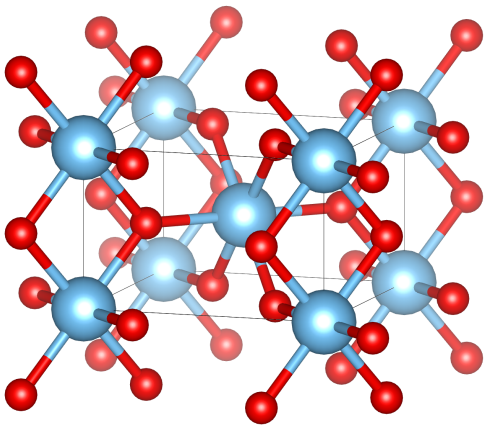

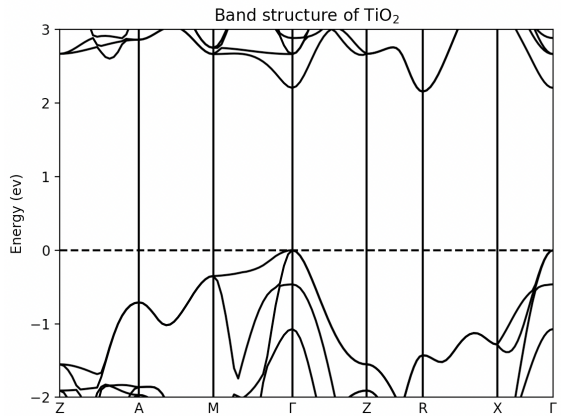

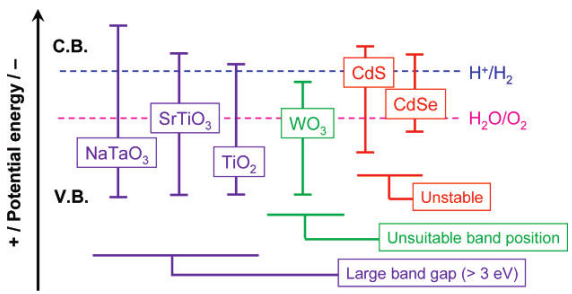

K. Maeda and K. Domen, J. Phys. Chem. C **111**, 7851–7861 (2007)

Band-gap problem in LDA/GGA

The fundamental band gap from experiment

$$
\begin{aligned}
E_{\mathrm{g}}^{\mathrm{fund}} &= \mathrm{IP}(N) - \mathrm{EA}(N) \\
\mathrm{IP}(N) &= E_0(N-1) - E_0(N) \\
&= -\lim_{\eta \to 0^+} \mu(N-\eta) \\
\mathrm{EA}(N) &= E_0(N+1) - E_0(N) \\
&= \lim_{\eta \to 0^+} \mu(N+\eta)
\end{aligned}
$$

For semiconductors

$$
E_{\mathrm{g}}^{\mathrm{KS}} = \epsilon_{\mathrm{CBM}}^{\mathrm{KS}} - \epsilon_{\mathrm{VBM}}^{\mathrm{KS}} \ll E_{\mathrm{g}}^{\mathrm{fund}}
$$

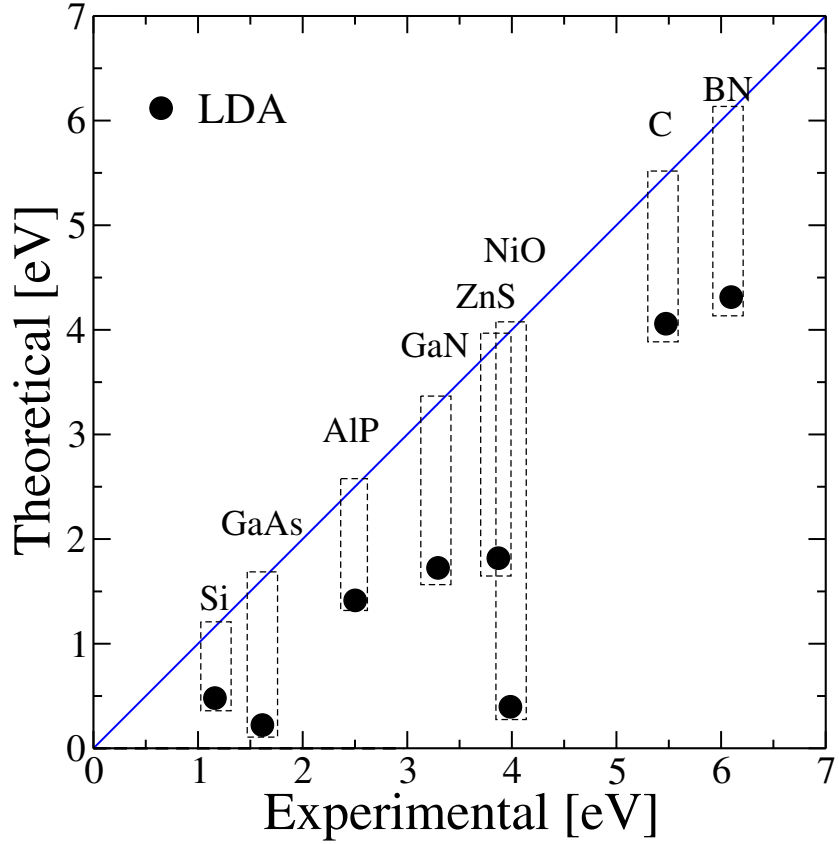

Picture courtesy: adapted from lecture note of Prof. Hong Jiang

Improving the band structure prediction in DFT

Underestimates stems from

- So-called derivative discontinuity $\Delta_{\mathrm{xc}} = 0$ for E_{xc} with explicit n, i.e. semi-local DFA
- Missing Δ_{xc} in the band structure, even E_{xc} is "exact"

Current solutions

- adding non-zero Δ_{xc} explicitly as a correction, e.g. GLLB-SC
- Incorporating Δ_{xc} inside the band: generalized Kohn-Sham theory, e.g. hybrid functionals

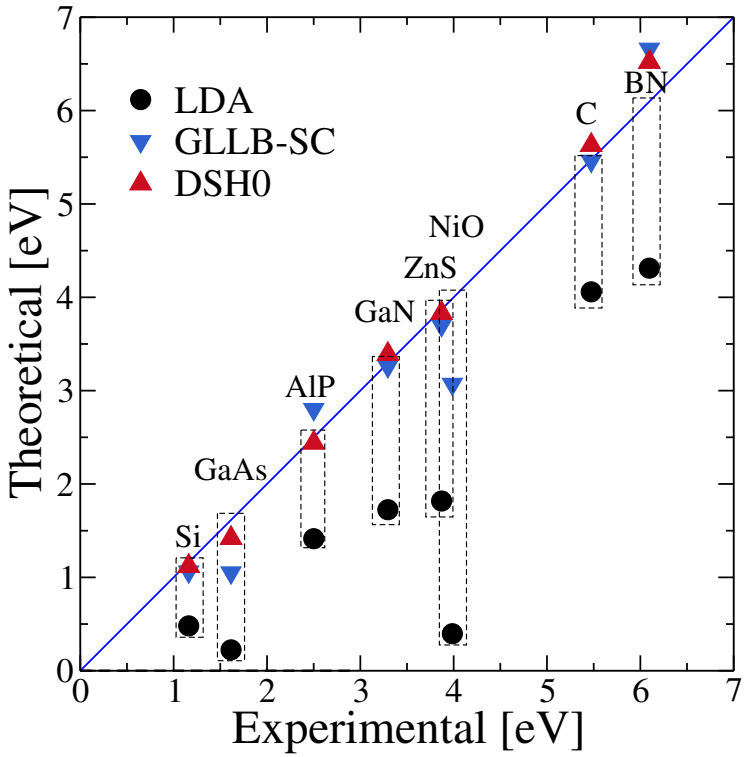

For derivation see E. Engel and R. M. Dreizler, *Density Functional Theory: An Advanced Course*, (Springer Science & Business Media, 2011), 543 pp., p37 and 99

F. Tran, S. Ehsan, and P. Blaha, Phys. Rev. Materials **2**, 023802 (2018)

Z.-H. Cui et al., J. Phys. Chem. Lett. **9**, 2338–2345 (2018), A. Seidl et al., Phys. Rev. B **53**, 3764–3774 (1996)

Go beyond DFT

- Hybrid functionals generally have tunable parameters obtained from fitting specific database, not that *ab initio* ...
- Even with system-dependent parameters, hybrid functional based on a model could fail in a "simple" system, e. g. FeS_2.
- Well, accurate enough, but not as far beyond as CCSD or even full CI ...

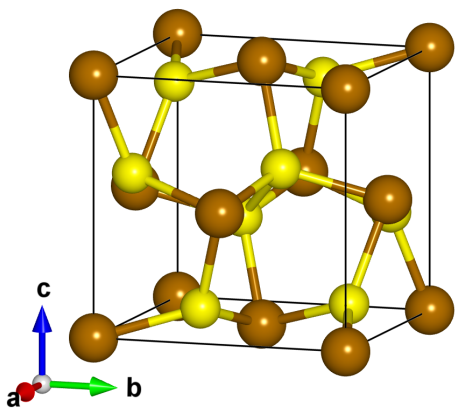

Non-magnetic, Fe in low-spin state.

	Expt.	PBE	PBE0	HSE06	DSH0
E_g	0.95	0.70	2.96	2.22	2.43

A. Ennaoui et al., Sol. Energy Mater. Sol. Cells **29**, 289–370 (1993), M.-Y. Zhang and H. Jiang, Front. Chem. **9**, 747972 (2021)

Outline

Green's function in many-body perturbation theory

The time-ordered Green's function

$$\mathrm{i}G_{\alpha\beta}\left(\mathbf{x}_1 t_1, \mathbf{x}_2 t_2\right) = \left\langle \Psi(N) \middle| \mathrm{T}\left\{ \hat{\psi}_\alpha\left(\mathbf{x}_1 t_1\right) \hat{\psi}^\dagger_\beta\left(\mathbf{r}_2 t_2\right) \right\} \middle| \Psi(N) \right\rangle$$

Its Lehnmann representation

$$G_{\alpha\beta}\left(\mathbf{x}_1, \mathbf{x}_2, \omega\right) = \sum_j \frac{p_{\alpha j}\left(\mathbf{x}_1\right) p^*_{\beta j}\left(\mathbf{x}_2\right)}{\omega - \omega_{N+1,j} + \omega_N + i\eta} + \sum_i \frac{h_{\alpha i}\left(\mathbf{x}_1\right) h^*_{\beta i}\left(\mathbf{x}_2\right)}{\omega - \omega_N + \omega_{N-1,i} - i\eta}$$

$\omega_{N\pm1,i}$: the total energy of i-th excited state of $N \pm 1$-electron system

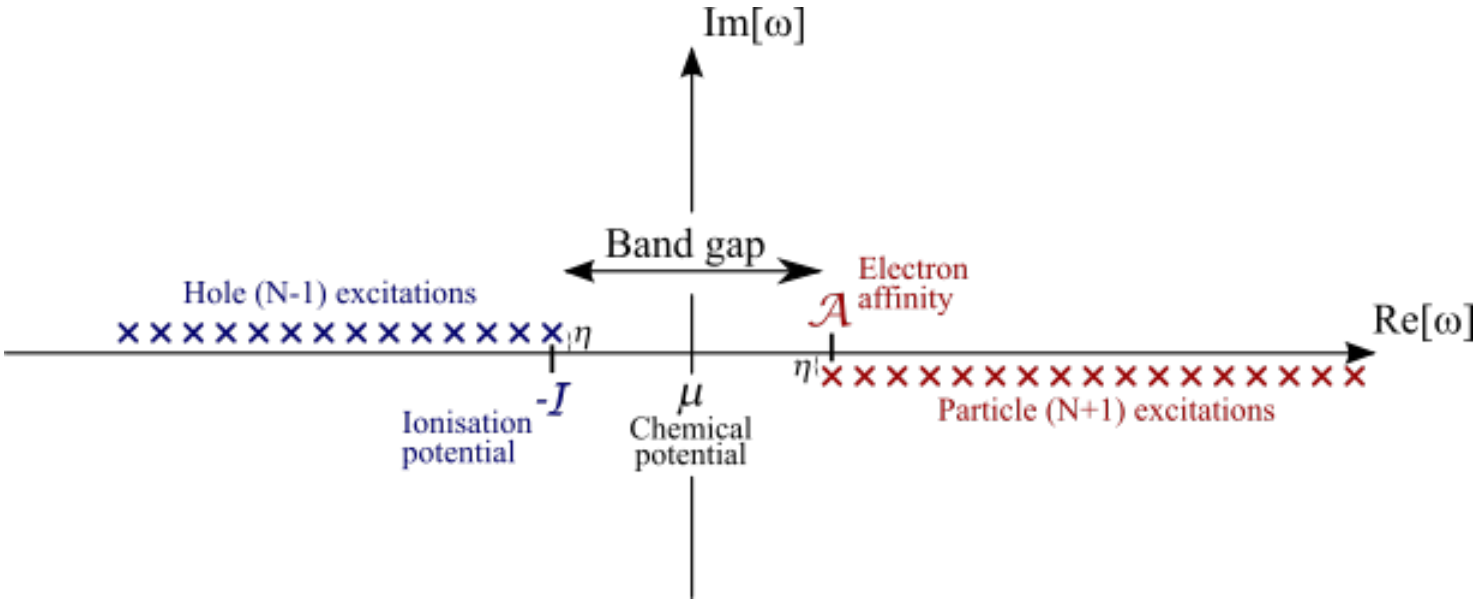

Picture courtsey: ABINIT project

Hedin's equations

With notation $1 \equiv (\mathbf{x}_1 t_1)$

$$\begin{cases} P(1,2) & = -\mathrm{i} \int \mathrm{d}(34)\, G(1,3)\Gamma(3,4,2)G(4,1^+) \\ W(1,2) & = v(1,2) + \int \mathrm{d}(34)\, v(1,3)P(3,4)W(4,2) \\ \Sigma(1,2) & = \mathrm{i} \int \mathrm{d}(34)\, G(1,3)W(4,1)\Gamma(3,2,4) \\ \Gamma(1,2,3) & = \delta(1,2)\delta(1,3) + \int \mathrm{d}(4567)\, \frac{\delta\Sigma(1,2)}{\delta G(4,5)} G(4,6)\Gamma(6,7,3)G(7,5) \\ G(1,2) & = G_0(1,2) + \int \mathrm{d}(3,4)\, G_0(1,3)\Sigma(3,4)G(4,2) \end{cases}$$

where $P := \delta n / \delta v_{\mathrm{tot}}$ is the polarization function, W the screened Coulomb interaction and Γ the vertex function.

L. Hedin, Phys. Rev. **139**, A796–A823 (1965). For a relatively modern and comprehensive derivation, see a note by Aryasetiawan, also F. Aryasetiawan and O. Gunnarsson, Rep. Prog. Phys. **61**, 237 (1998) and D. Golze, M. Dvorak, and P. Rinke, Front. Chem. **7**, 377 (2019)

Quasiparticle equation

Alternatively, one can get the excitation energies by solving

$$[t_{\mathbf{x}} + v_{\mathrm{ext}}(\mathbf{x}) + v_{\mathrm{H}}(\mathbf{x})]\,\Phi_n(\mathbf{x},\omega) + \int \mathrm{d}\mathbf{x}'\Sigma(\mathbf{x},\mathbf{x}',\omega)\Phi_n(\mathbf{x}') = \epsilon_n(\omega)\Phi_n(\mathbf{x},\omega)$$

If we focus on the solutions satisfying $\omega = \epsilon_n(\omega)$ and $\mathrm{Im}\,\epsilon_n(\omega) \approx 0$, i.e. quaisparticle,

$$[t_{\mathbf{x}} + v_{\mathrm{ext}}(\mathbf{x}) + v_{\mathrm{H}}(\mathbf{x})]\,\Phi_n(\mathbf{x}) + \int \mathrm{d}\mathbf{x}'\Sigma(\mathbf{x},\mathbf{x}',\epsilon_n^{\mathrm{QP}})\Phi_n(\mathbf{x}') = \epsilon_n^{\mathrm{QP}}\Phi_n(\mathbf{x})$$

where ϵ_n^{QP} are the quasiparticle energies.

F. Aryasetiawan and O. Gunnarsson, Rep. Prog. Phys. **61**, 237 (1998), L. Hedin, Phys. Rev. **139**, A796–A823 (1965)

GW approximation

Drop the complicated second term in the vertex function,

$$\begin{cases} P &= -\mathrm{i}GG\Gamma G \\ W &= v + vPW \\ \Sigma &= \mathrm{i}GW\Gamma \\ \Gamma &= \hat{1} + \frac{\delta\Sigma}{\delta G}GG\Gamma G \\ G &= G_0 + G_0\Sigma G \end{cases} \Longrightarrow \begin{cases} P &= -\mathrm{i}GG \\ W &= v + vPW \\ \Sigma &= \mathrm{i}GW \\ G &= G_0 + G_0\Sigma G \end{cases}$$

Variants: non-self-consistent G_0W_0, GW_0, self-consistent GW...

Hedin's equation in diagrams

$v(1,2) =$ 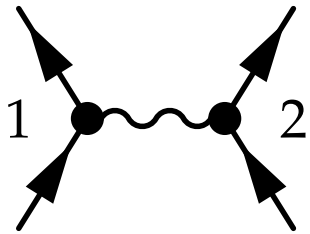

$W(1,2) =$ 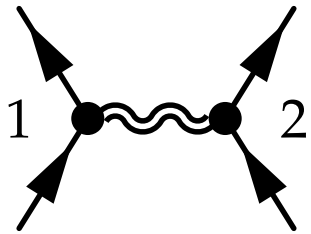

$P(1,2) =$ 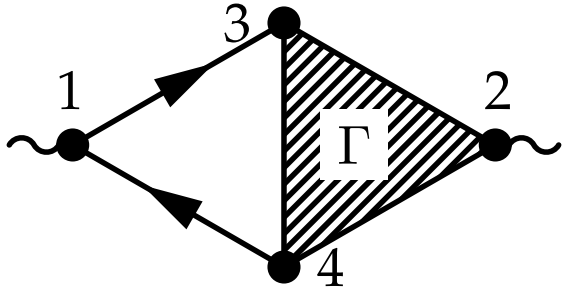

$\Sigma(1,2) =$ 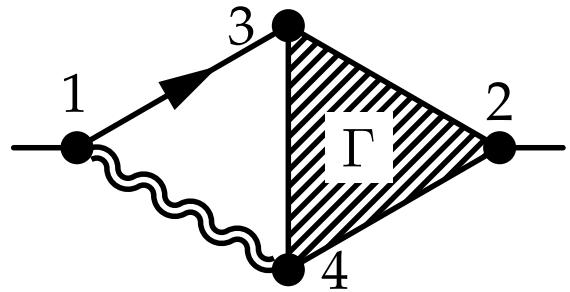

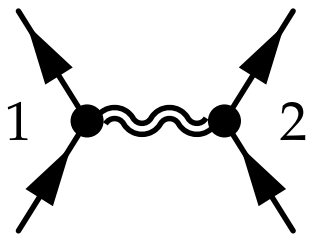

$=$ 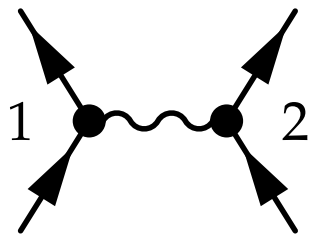

$+$ 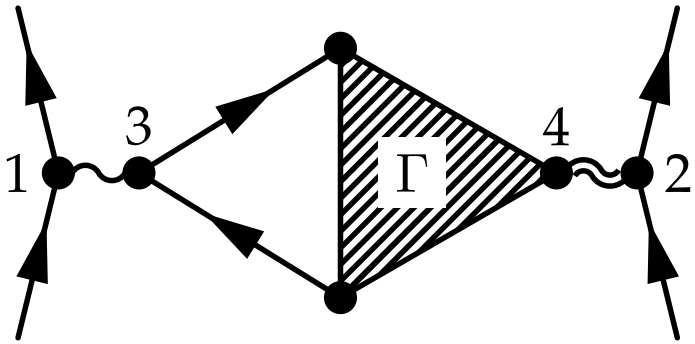

$\Gamma(1,2,3) =$ 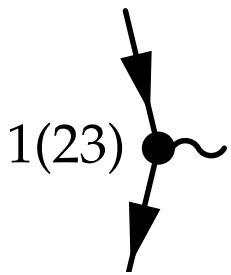

$+$ 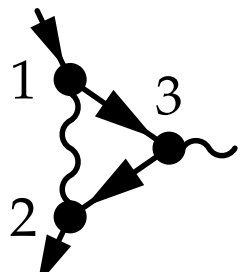

$+ \cdots$

GW approximation in diagrams

$P(1,2) =$ 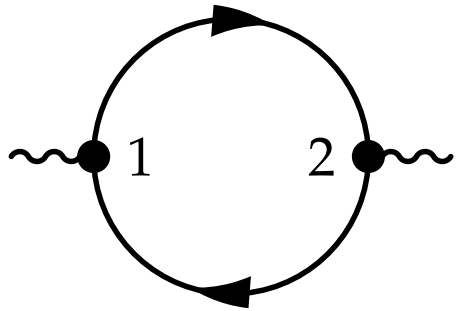

$\Sigma(1,2) =$ 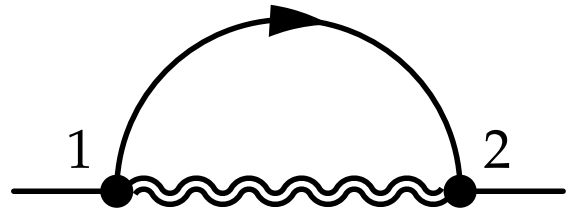

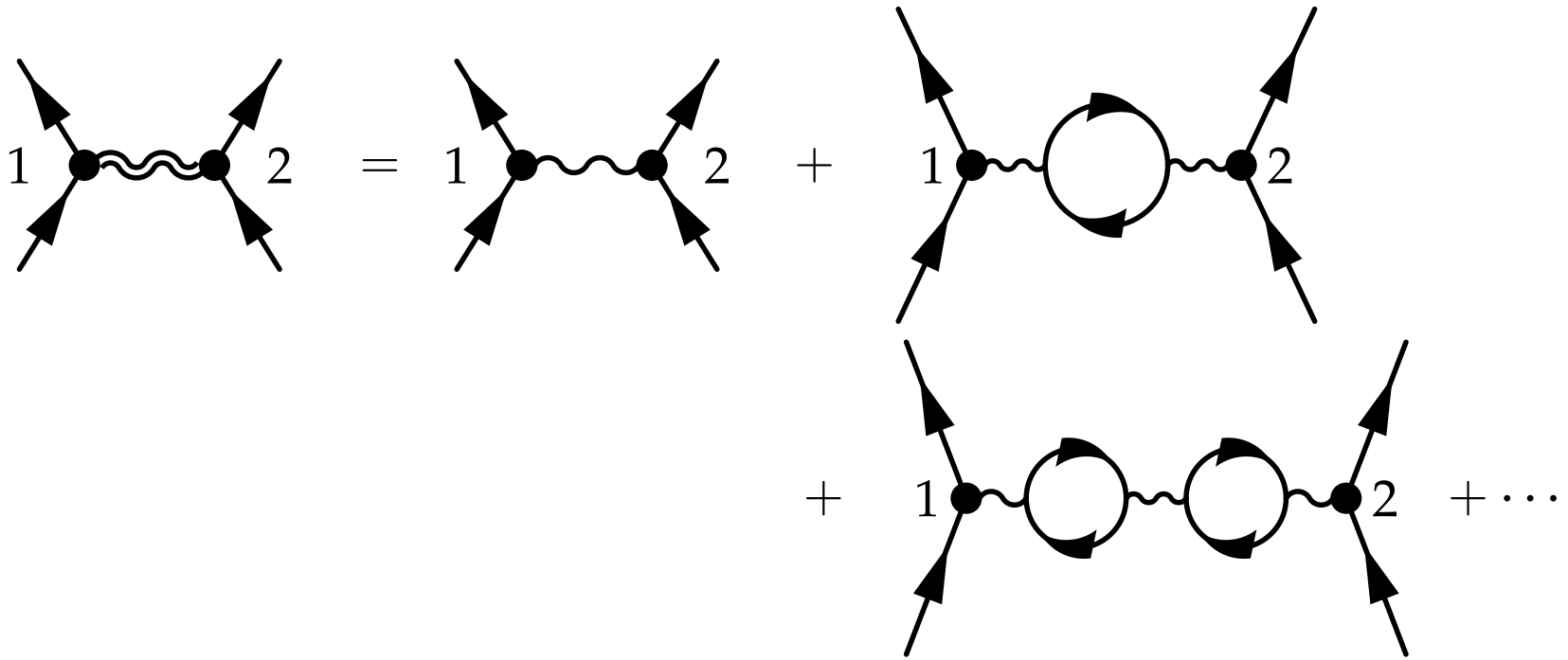

G_0W_0: the most popular variant

$$\Sigma(\mathbf{r},\mathbf{r}',\omega) = \frac{\mathrm{i}}{2\pi}\int_{-\infty}^{\infty} \mathrm{d}\omega' \mathrm{e}^{\mathrm{i}\omega'\delta} G_0(\mathbf{r},\mathbf{r}',\omega+\omega') W_0(\mathbf{r}',\mathbf{r},\omega')$$

$$G_0\left(\mathbf{r},\mathbf{r}',\omega\right) = \sum_{n\mathbf{k}} \frac{\psi_{n\mathbf{k}}\left(\mathbf{r}\right)\psi^*_{n\mathbf{k}}\left(\mathbf{r}'\right)}{\omega - \epsilon^{\mathrm{KS}}_{n\mathbf{k}} - \mathrm{i}\eta\mathrm{sgn}\left(\mu - \epsilon^{\mathrm{KS}}_{n\mathbf{k}}\right)}$$

$$W_0(\mathbf{r},\mathbf{r}',\omega) = \int \mathrm{d}\mathbf{r}''\, \varepsilon_0^{-1}(\mathbf{r},\mathbf{r}'',\omega) v(\mathbf{r}'',\mathbf{r}')$$

$$\boldsymbol{\varepsilon}_0(\omega) = \mathbf{1} - \mathbf{v}\mathbf{P}_0(\omega) = \mathbf{1} - \mathbf{v}\boldsymbol{\chi}_0(\omega)$$

$$\boldsymbol{\chi}_0(\omega) = -\frac{\mathrm{i}}{2\pi}\int_{-\infty}^{\infty} \mathrm{d}\omega' \mathrm{e}^{\mathrm{i}\omega'\delta} \mathbf{G}_0(\omega+\omega')\mathbf{G}_0(\omega')$$

M. S. Hybertsen and S. G. Louie, Phys. Rev. B **34**, 5390–5413 (1986), M. Shishkin and G. Kresse, Phys. Rev. B **75**, 235102 (2007), M. Usuda et al., Phys. Rev. B **66**, 125101 (2002)

Conventional *GW* implementation

$$M^{\mu}_{nm}(\mathbf{k},\mathbf{q}) = \sqrt{N_k}\int_V \mathrm{d}\mathbf{r}\left[P^{\mathbf{q}}_{\mu}(\mathbf{r})\psi_{m\mathbf{k}-\mathbf{q}}(\mathbf{r})\right]^*\psi_{n\mathbf{k}}(\mathbf{r})$$

$$P_{\mu\nu}(\mathbf{q},\omega) = \frac{1}{\Omega}\sum_{\mathbf{k}}\sum_{nm}F_{nm}(\mathbf{k},\mathbf{q},\omega)M^{\mu}_{nm}(\mathbf{k},\mathbf{q})\left[M^{\nu}_{nm}(\mathbf{k},\mathbf{q})\right]^*$$

$$F_{nm}(\mathbf{k},\mathbf{q},\omega) = 2f_{n\mathbf{k}}\left(1-f_{m\mathbf{k}-\mathbf{q}}\right)\left\{\frac{1}{\omega-\epsilon_{m\mathbf{k}-\mathbf{q}}+\epsilon_{n\mathbf{k}}+\mathrm{i}\eta}-\frac{1}{\omega+\epsilon_{m\mathbf{k}-\mathbf{q}}-\epsilon_{n\mathbf{k}}-\mathrm{i}\eta}\right\}$$

$$\Sigma^{\mathrm{x}}_{n\mathbf{k}} = -\frac{1}{N_k}\sum_{\mathbf{q}}\sum_{\mu}v_{\mu}(\mathbf{q})\sum_{m}f_{m\mathbf{k}-\mathbf{q}}|M^{\mu}_{mn}(\mathbf{k},\mathbf{q})|^2 \text{ (exact exchange, EXX)}$$

$$\Sigma^{\mathrm{c}}_{n\mathbf{k}}(\omega) = \frac{\mathrm{i}}{2\pi N_k}\int_{-\infty}^{\infty}\mathrm{d}\omega'\sum_{m}\sum_{\mathbf{q}}\frac{X_{nm}(\mathbf{k},\mathbf{q},\omega')}{\omega+\omega'-\epsilon_{m\mathbf{k}-\mathbf{q}}+\mathrm{i}\eta\mathrm{sgn}\left(\epsilon_{m\mathbf{k}-\mathbf{q}}-\mu\right)}$$

$$X_{nm}(\mathbf{k},\mathbf{q},\omega) = \sum_{\mu\nu}\left[v_{\mu}(\mathbf{q})M^{\mu}_{nm}(\mathbf{k},\mathbf{q})\right]^*\left[\varepsilon_{\mu\nu}(\mathbf{q},\omega)-1\right]v_{\nu}(\mathbf{q})M^{\nu}_{nm}(\mathbf{k},\mathbf{q})$$

- Auxiliary basis $P^{\mathbf{q}}_{\mu}(\mathbf{r})$: plane-wave, NAO, GTO, mixed basis, ...
- $\sum nm$: high-lying states, basis-set completeness ...
- Frequency integration $\int \mathrm{d}\omega$: plasmon-pole model, full frequency, ...
- $v_{\mu}(\mathbf{q})$: bare or (1/2/3D-)truncated Coulomb kernel ...

Overview of *GW* data flow: example in LAPW

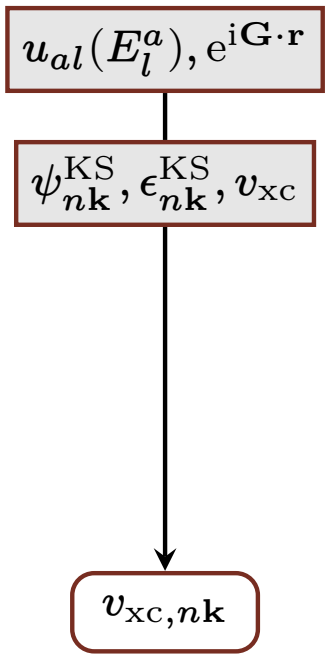

Use DFT program (WIEN2K in this case) to obtain

- basis functions
- groundstate KS energies and wave-functions
- XC potential

H. Jiang et al., Comput. Phys. Commun. **184**, 348–366 (2013)

Overview of *GW* data flow: example in LAPW

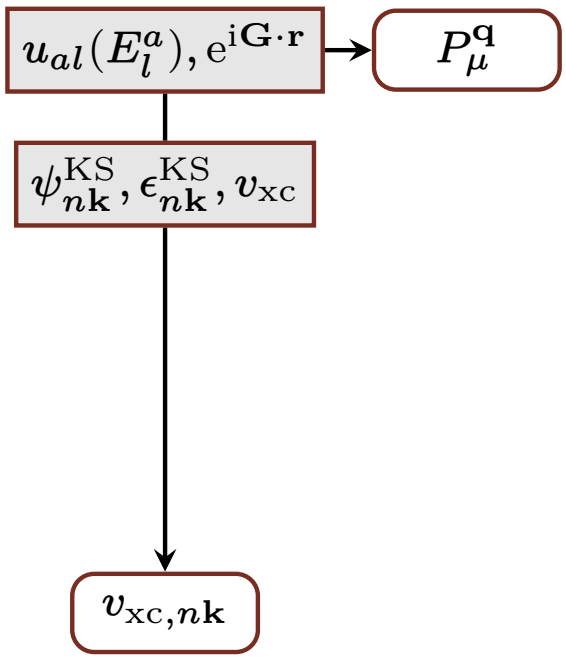

Mixed basis (MPB) as auxiliary basis for expanding $\psi^*\psi$ by diagonalize overlap matrix of

- MT: radial functions in each L channel

$$u_{nl}(r, E_{nl}^a)u_{n'l'}(r, E_{n'l'}^a)$$

  satisfying $|l - l'| \leq L \leq |l + l'|$

- interstial: IPW up to $2K_{\max}$

Eigenpairs with eigenvalues below a threshold are discarded.

F. Aryasetiawan and O. Gunnarsson, Phys. Rev. B **49**, 16214–16222 (1994)
H. Jiang et al., Comput. Phys. Commun. **184**, 348–366 (2013)

Overview of *GW* data flow: example in LAPW

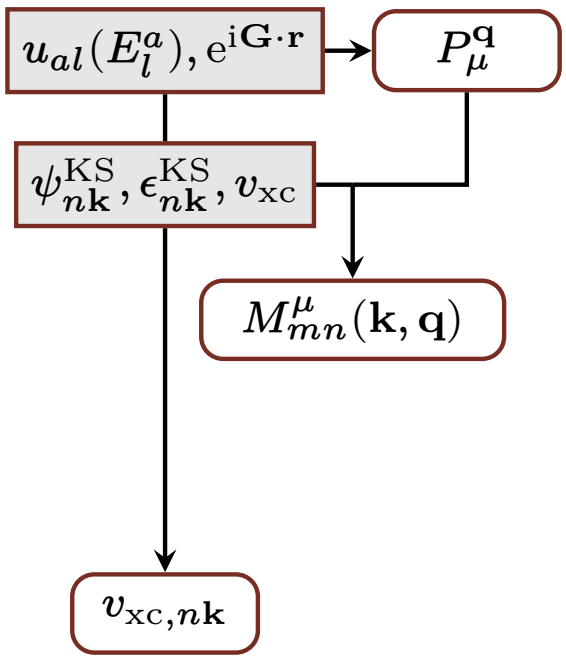

Projection of $\psi^*\psi$ out of MPB

$$M_{nm}^{\mu}(\mathbf{k},\mathbf{q}) = \int_V \mathrm{d}\mathbf{r}\left[P_\mu^{\mathbf{q}}(\mathbf{r})\psi_{m\mathbf{k}-\mathbf{q}}(\mathbf{r})\right]^* \psi_{n\mathbf{k}}(\mathbf{r})$$

H. Jiang et al., Comput. Phys. Commun. **184**, 348–366 (2013)

Overview of *GW* data flow: example in LAPW

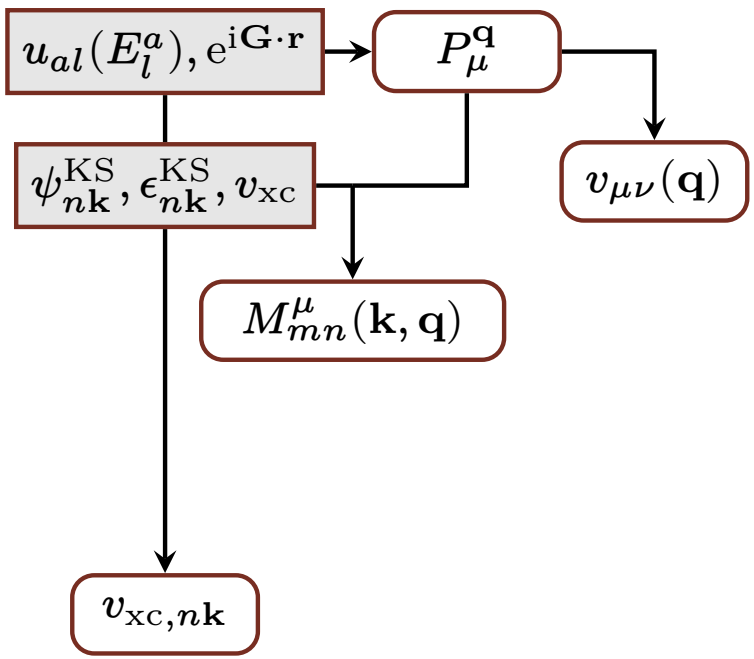

Coulomb matrix element

- MT-MT: compute a Ewald-like lattice sum

$$\Sigma_{\lambda\mu}^{a,a'}(\mathbf{q}) = \sum_{\mathbf{R}} \frac{\mathrm{e}^{\mathrm{i}\mathbf{q}\cdot\mathbf{R}_{aa'}}}{\bar{R}_{aa'}^{\lambda}} Y_{\lambda\mu}(\hat{\mathbf{R}}_{aa'})$$

- MT-IPW or IPW-IPW: use PW representation $v_{\mathbf{G}\mathbf{G}'}$

$$v_{\mathbf{G}\mathbf{G}'}(\mathbf{q}) = \delta_{\mathbf{G}\mathbf{G}'} \frac{4\pi}{|\mathbf{q}+\mathbf{G}|^2}$$

- Rotate auxiliary basis $P_\mu^{\mathbf{q}}$ to be v-diagonal

B. R. A. Nijboer and F. W. De Wette, Physica **23**, 309–321 (1957)
H. Jiang et al., Comput. Phys. Commun. **184**, 348–366 (2013)

Overview of *GW* data flow: example in LAPW

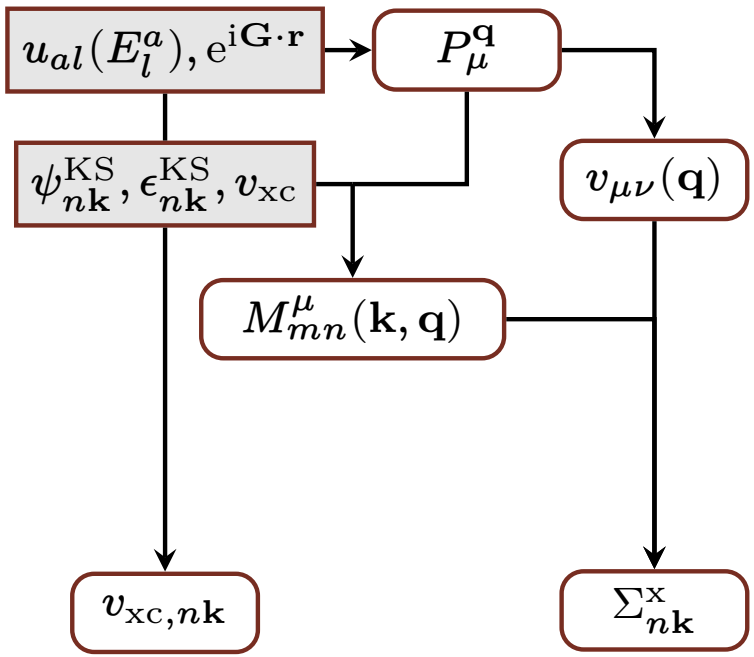

Exchange self-energy

$$\Sigma_{n\mathbf{k}}^{\mathrm{x}} = -\frac{1}{N_k}\sum_{\mathbf{q}}\sum_{\mu}\sum_{n'\in\mathrm{occ.}} \left|M_{nn'}^{\mu}(\mathbf{k},\mathbf{q})\right|^2 v_\mu(\mathbf{q})$$

Gygi-Baldereschi scheme is used to address Coulomb divergence for $\mathbf{q}\to 0$

F. Gygi and A. Baldereschi, Phys. Rev. B **34**, 4405–4408 (1986), S. Massidda, M. Posternak, and A. Baldereschi, Phys. Rev. B **48**, 5058–5068 (1993)

H. Jiang et al., Comput. Phys. Commun. **184**, 348–366 (2013)

Overview of *GW* data flow: example in LAPW

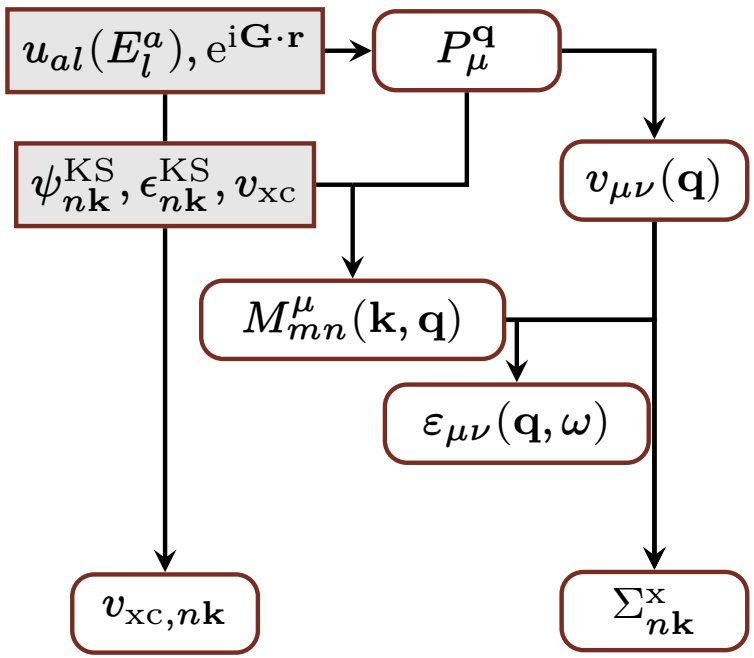

Symmetrized dielectric matrix. For gapped systems,

$$\varepsilon_{\mu\nu}(\mathbf{q},\omega) = \delta_{\mu\nu} - \frac{1}{N_k} \sum_{\mathbf{q}} \sum_{\substack{n\in\mathrm{occ.}\\ m\in\mathrm{vir.}}} \sqrt{v_\mu(\mathbf{q}) v_\nu(\mathbf{q})}\, F_{nm\mathbf{k}}(\mathbf{q},\omega) \left[M_{nm}^{\mu}(\mathbf{k},\mathbf{q})\right]^* M_{nm}^{\nu}(\mathbf{k},\mathbf{q})$$

where

$$F_{nm\mathbf{k}}(\omega) = \frac{1}{\omega - \epsilon_{m\mathbf{k}-\mathbf{q}} + \epsilon_{n\mathbf{k}} + i\eta} - \frac{1}{\omega + \epsilon_{m\mathbf{k}-\mathbf{q}} - \epsilon_{n\mathbf{k}} - i\eta}$$

H. Jiang et al., Comput. Phys. Commun. **184**, 348–366 (2013)

Overview of *GW* data flow: example in LAPW

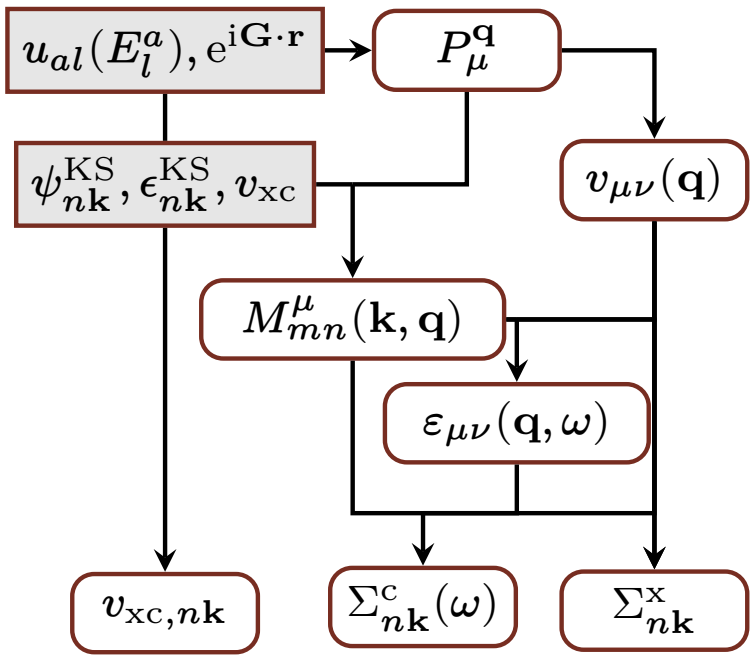

Correlation self-energy on imaginary frequency $\omega = \mathrm{i}u$

$$\Sigma_{n\mathbf{k}}^{\mathrm{c}}(\mathrm{i}u) = -\frac{1}{N_k}\sum_{\mathbf{q}}\sum_{\mu\nu,m}\int\frac{\mathrm{d}u'}{2\pi}\left[\varepsilon_{\mu\nu}^{-1}(\mathbf{q},\mathrm{i}u')-1\right] \times \frac{v_\mu(\mathbf{q})\left[M_{nm}^{\mu}(\mathbf{k},\mathbf{q})\right]^* v_\nu(\mathbf{q}) M_{nm}^{\nu}(\mathbf{k},\mathbf{q})}{\mathrm{i}u+\mathrm{i}u'-\epsilon_{m\mathbf{k}+\mathbf{q}}}$$

and then analytically continued to real axis by using e.g. Padé approximant.

H. N. Rojas, R. W. Godby, and R. J. Needs, Phys. Rev. Lett. **74**, 1827 (1995)
H. Jiang et al., Comput. Phys. Commun. **184**, 348–366 (2013)

Overview of *GW* data flow: example in LAPW

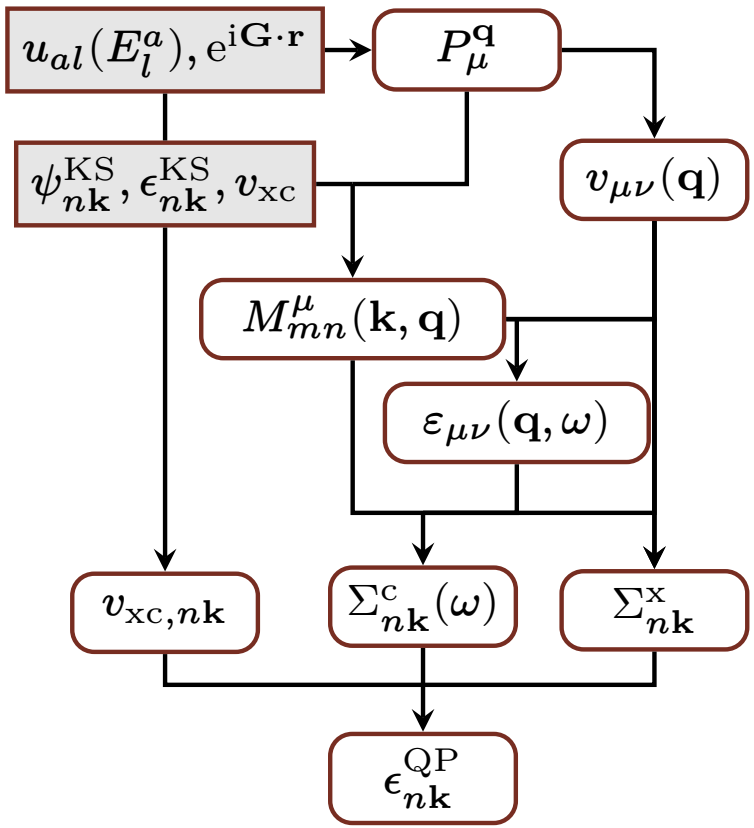

Solve the quasi-particle equation to obtain quasi-particle energy ϵ^{QP}

$$\omega = \epsilon_{n\mathbf{k}}^{\mathrm{KS}} + \mathrm{Re}\ \langle n\mathbf{k}|\Sigma(\omega) - v^{\mathrm{xc}}|n\mathbf{k}\rangle$$

Perturbation treatment

$$\begin{aligned}\epsilon_{n\mathbf{k}}^{\mathrm{QP}} \approx & \epsilon_{n\mathbf{k}}^{\mathrm{KS}} + \Sigma_{n\mathbf{k}}(\epsilon_{n\mathbf{k}}^{\mathrm{KS}}) + (\epsilon_{n\mathbf{k}}^{\mathrm{QP}} - \epsilon_{n\mathbf{k}}^{\mathrm{KS}})\Sigma'_{n\mathbf{k}}(\epsilon_{n\mathbf{k}}^{\mathrm{KS}}) \\ & - v_{n\mathbf{k}}^{\mathrm{xc}} \\ = & \epsilon_{n\mathbf{k}}^{\mathrm{KS}} + \underbrace{\left[1 - \Sigma'_{n\mathbf{k}}(\epsilon_{n\mathbf{k}}^{\mathrm{KS}})\right]^{-1}}_{Z_{n\mathbf{k}}} \left[\Sigma_{n\mathbf{k}}(\epsilon_{n\mathbf{k}}^{\mathrm{KS}}) - v_{n\mathbf{k}}^{\mathrm{xc}}\right]\end{aligned}$$

Self-energy correction

$$\Delta\epsilon_{n\mathbf{k}}^{\mathrm{QP}} \overset{\mathrm{def}}{=} \epsilon_{n\mathbf{k}}^{\mathrm{QP}} - \epsilon_{n\mathbf{k}}^{\mathrm{KS}}$$

H. Jiang et al., Comput. Phys. Commun. **184**, 348–366 (2013)

Periodic *GW* in FHI-aims

Main difference from the LAPW implementaion

- (Localized) resolution of identity based on Coulomb metric

$$V_{\mu\nu}(\mathbf{q}) = \int \mathrm{d}\mathbf{r}\,\mathrm{d}\mathbf{r}'\,\frac{P_\mu^{\mathbf{q}}(\mathbf{r})P_\nu^{\mathbf{q}*}(\mathbf{r}')}{|\mathbf{r}-\mathbf{r}'|}$$

$$C_{ij}^{\mu} = \sum_{\nu}(ij|\nu)\left(V^{-1}\right)_{\nu\mu}$$

  where each of the auxiliary bases $P_\mu^{\mathbf{q}}$ is a Bloch sum of atom-centered function (product of NAOs).

- Truncated Coulomb kernel for building self-energy for better converging k points

$$v(r) = \frac{\mathrm{erfc}(\gamma r)}{r} + \frac{1}{2}\frac{\mathrm{erf}(\gamma r)}{r}\mathrm{erfc}\left[\frac{\ln(r)-\ln(R_{\mathrm{cut}})}{\ln(R_{\mathrm{w}})}\right]$$

  R_{cut} is determined by the inscribed sphere of the Born-von Karman cell. Bare-Coulomb limit is approximated with denser k grids.

X. Ren et al., Phys. Rev. Materials **5**, 013807 (2021)

Outline

GW in "real" systems

G_0W_0 and GW_0@PBE,
PAW/plane-wave

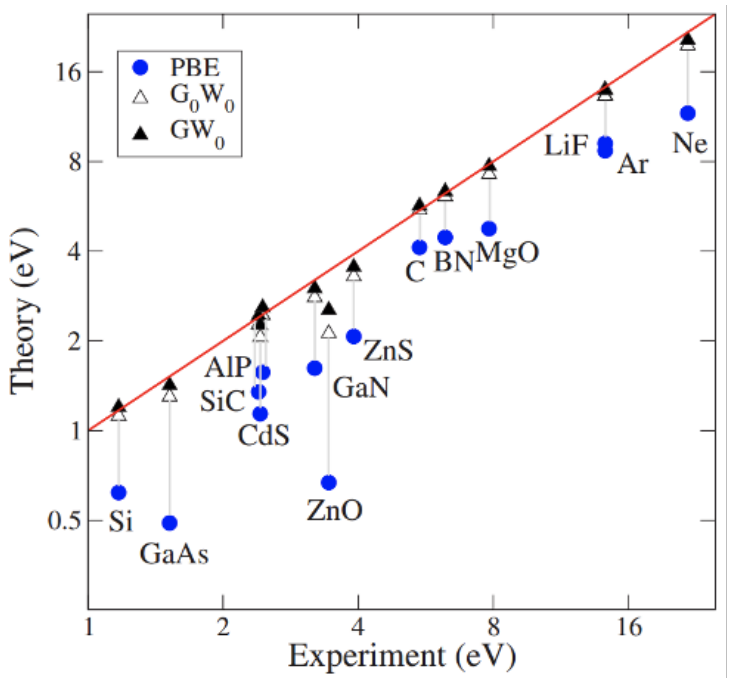

Quasi-particle self-consistent *GW*,
all-electron/LMTO

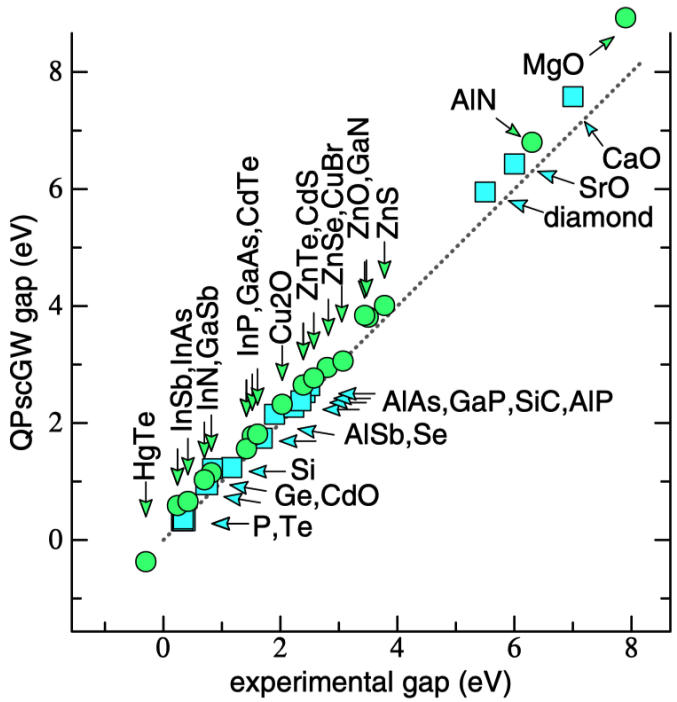

M. Shishkin and G. Kresse, Phys. Rev. B **75**, 235102 (2007)
M. van Schilfgaarde, T. Kotani, and S. Faleev, Phys. Rev. Lett. **96**, 226402 (2006)

GW in "real" systems

GW_0@PBE, all-electron/LAPW

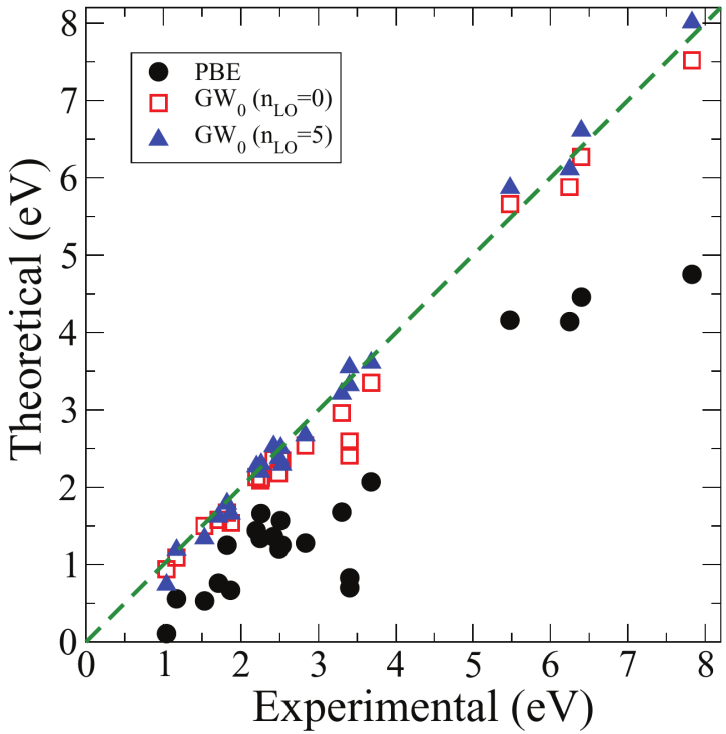

G_0W_0@PBE, all-electron/NAO

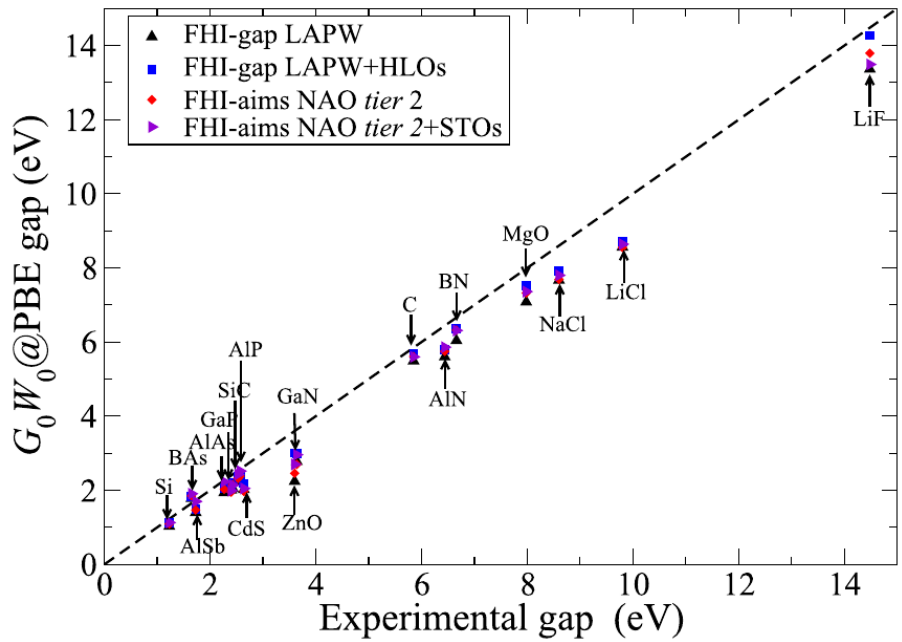

H. Jiang and P. Blaha, Phys. Rev. B **93**, 115203 (2016)
X. Ren et al., Phys. Rev. Materials **5**, 013807 (2021)

Effect of auxiliary basis in FHI-aims

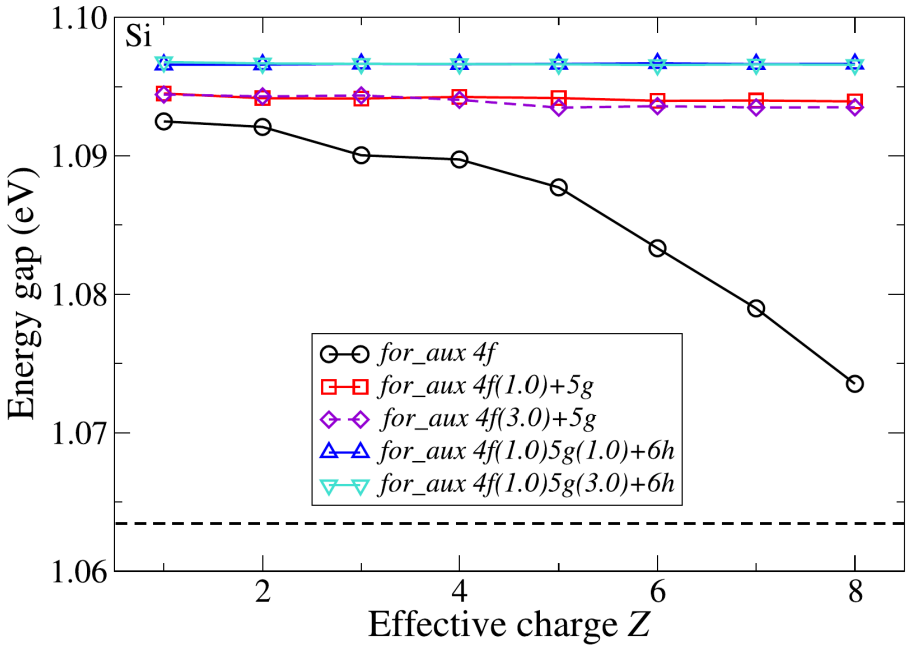

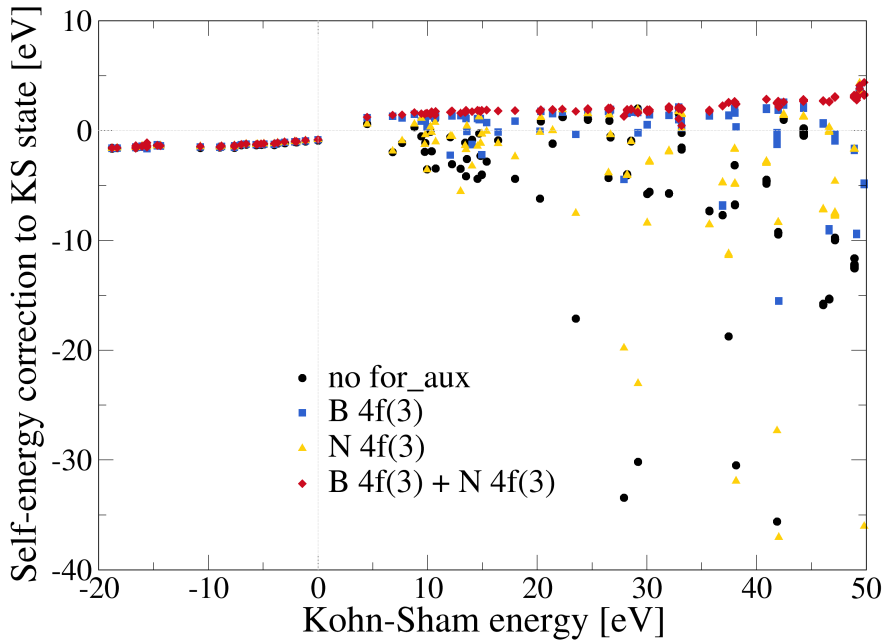

Source of error in $\Sigma^{c}_{n\mathbf{k}}$:

$$X_{nm}(\mathbf{k},\mathbf{q},\omega) = \sum_{\mu\nu} \left[v_\mu(\mathbf{q}) M^\mu_{nm}(\mathbf{k},\mathbf{q})\right]^* \left[\varepsilon_{\mu\nu}(\mathbf{q},\omega) - 1\right] v_\nu(\mathbf{q}) M^\nu_{nm}(\mathbf{k},\mathbf{q})$$

for high-lying unoccupied m state.

X. Ren et al., Phys. Rev. Materials **5**, 013807 (2021)

Zinc oxide puzzle

Band gap of ZnO has been heatedly debated since early 2000s.

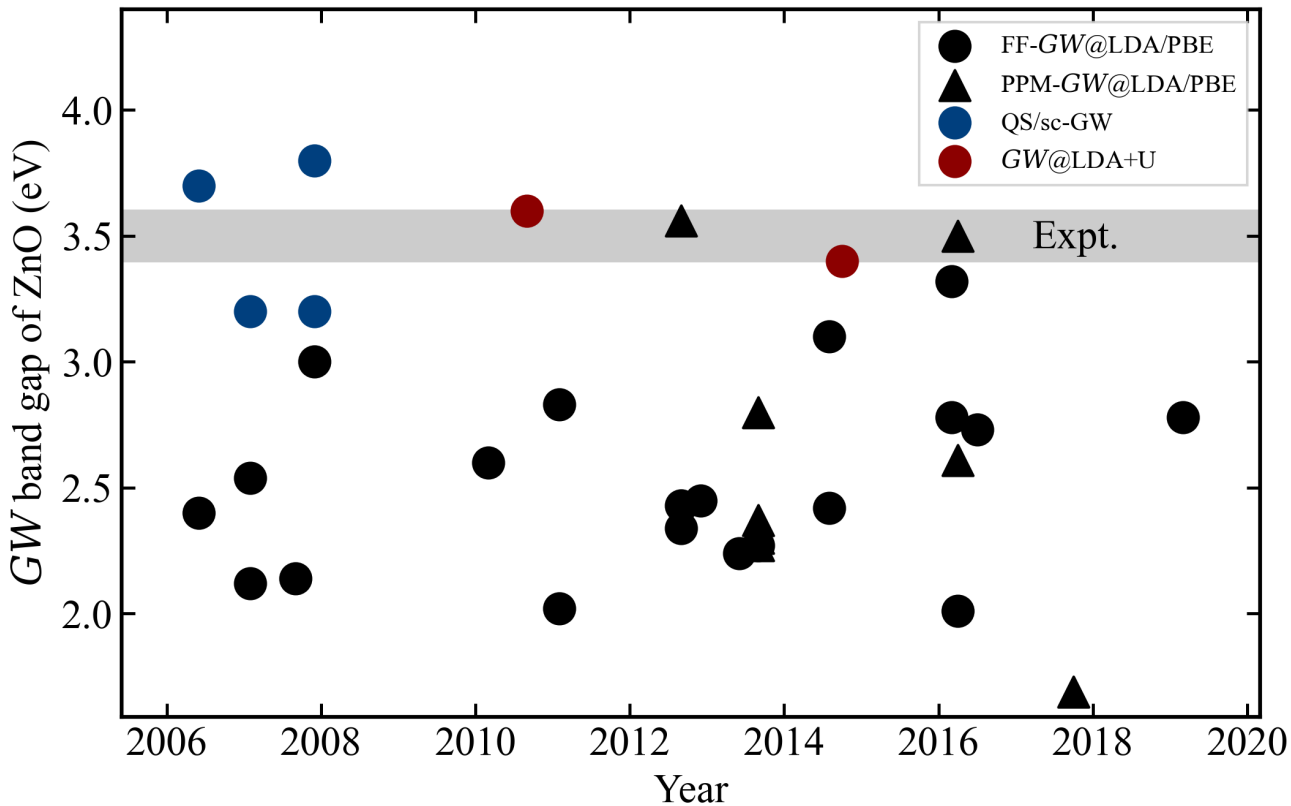

See e.g. M. van Schilfgaarde, T. Kotani, and S. V. Faleev, Phys. Rev. B **74**, 245125 (2006)

Basis set issue in ZnO QP gap

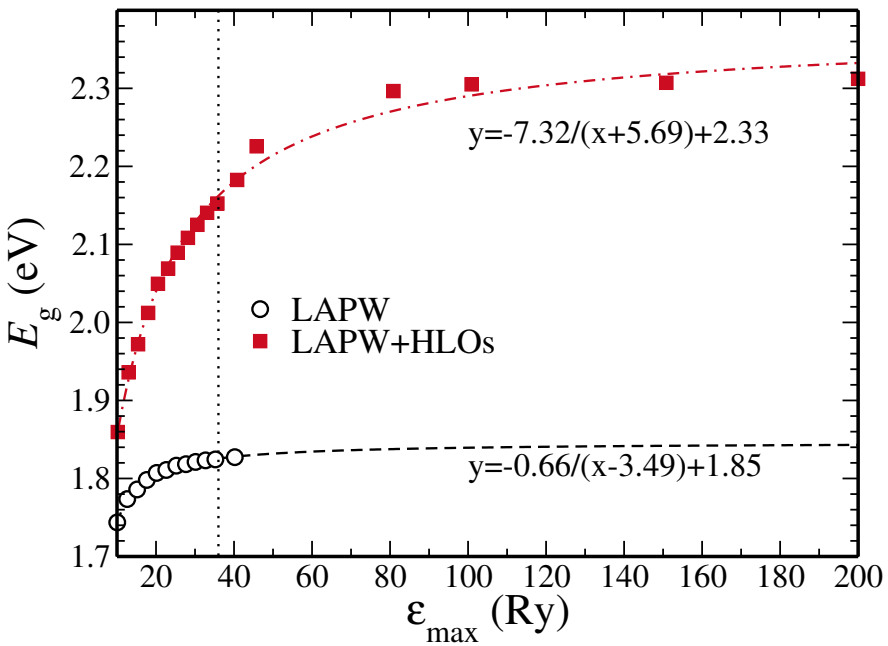

An improved basis set by introducing LOs at hight energy

- describes the unoccupied states more accurately
- offers a more complete space for sum of states

	PBE	LAPW		LAPW+HLOs		NC-PAW	Expt.
		G_0W_0	GW_0	G_0W_0	GW_0		
zb-ZnO	0.70	2.05	2.41	2.78	3.32		
wz-ZnO	0.83	2.24	2.59	3.01	3.55	3.4	3.4

H. Jiang and P. Blaha, Phys. Rev. B **93**, 115203 (2016), PAW from J. Klimeš, M. Kaltak, and G. Kresse, Phys. Rev. B **90**, 075125 (2014)

Tackling FeS_2 with *GW* in LAPW

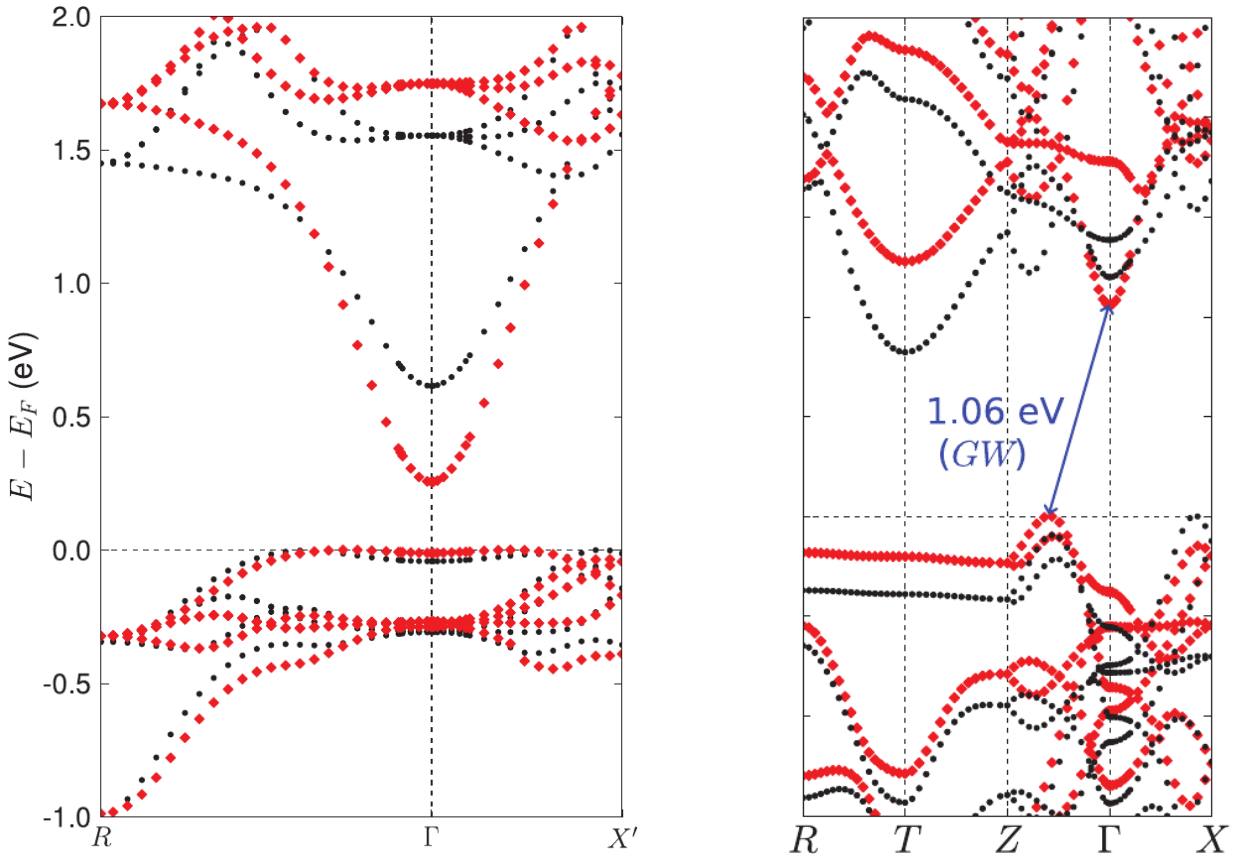

PBE vs G_0W_0@PBE

T. Schena, G. Bihlmayer, and S. Blügel, Phys. Rev. B **88**, 235203 (2013)

Complement the basis with extra LOs

Pyrite and marcasite phases of FeS_2

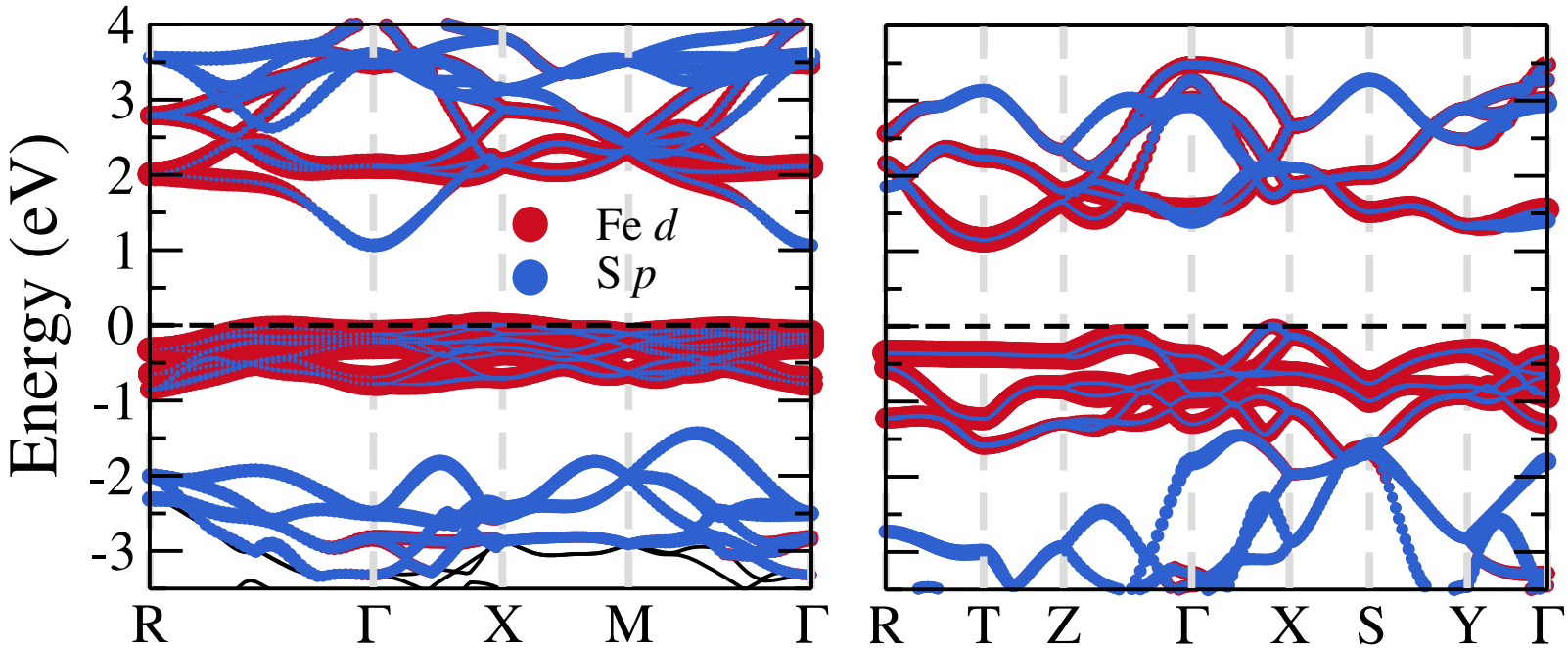

- Fe-3*d* as top valence bands
- Γ_c as an exclusive S-S anti-bonding state
- multiple low-energy conduction states in marcasite

M.-Y. Zhang and H. Jiang, Front. Chem. **9**, 747972 (2021)

QP band structure

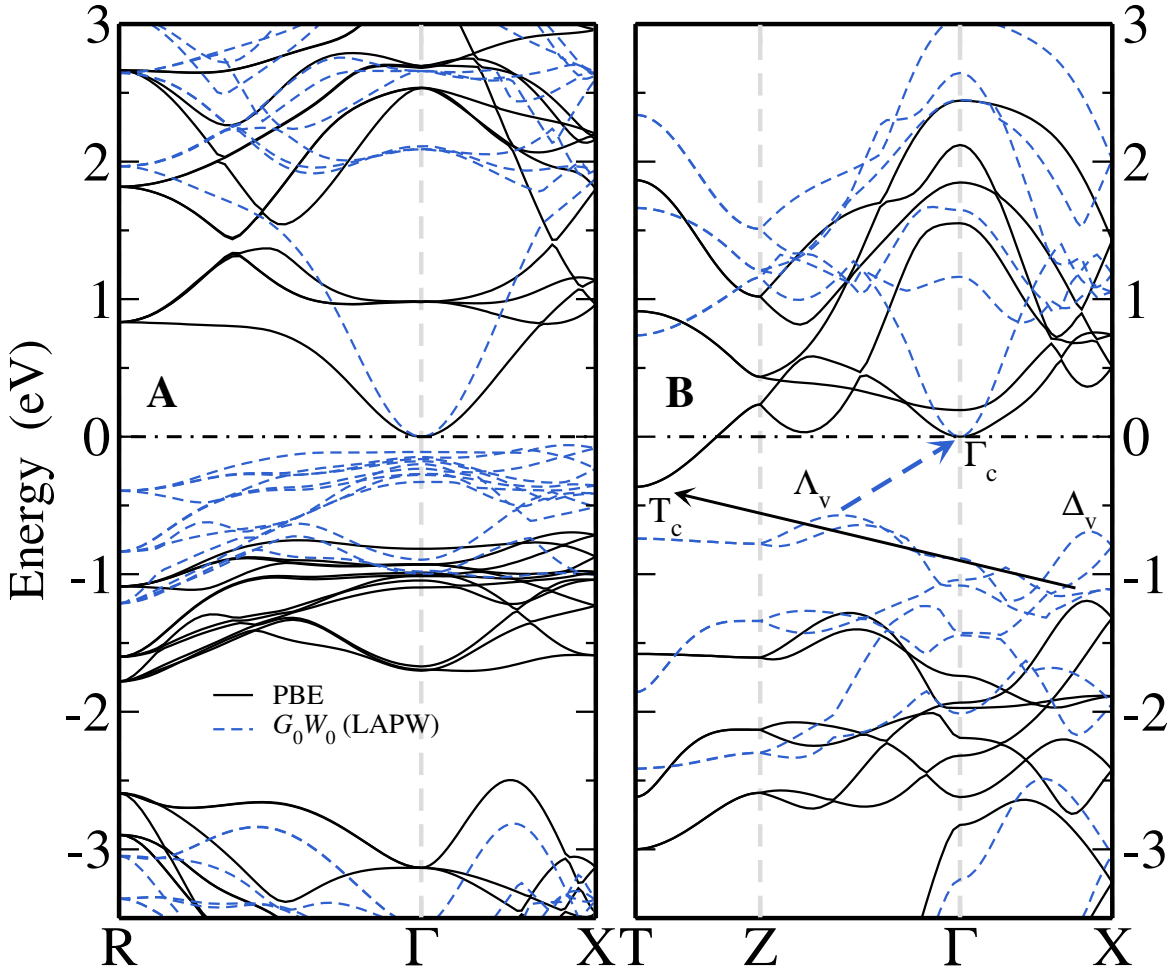

A: pyrite phase, B: marcasite phase

M.-Y. Zhang and H. Jiang, Front. Chem. **9**, 747972 (2021)

QP band structure

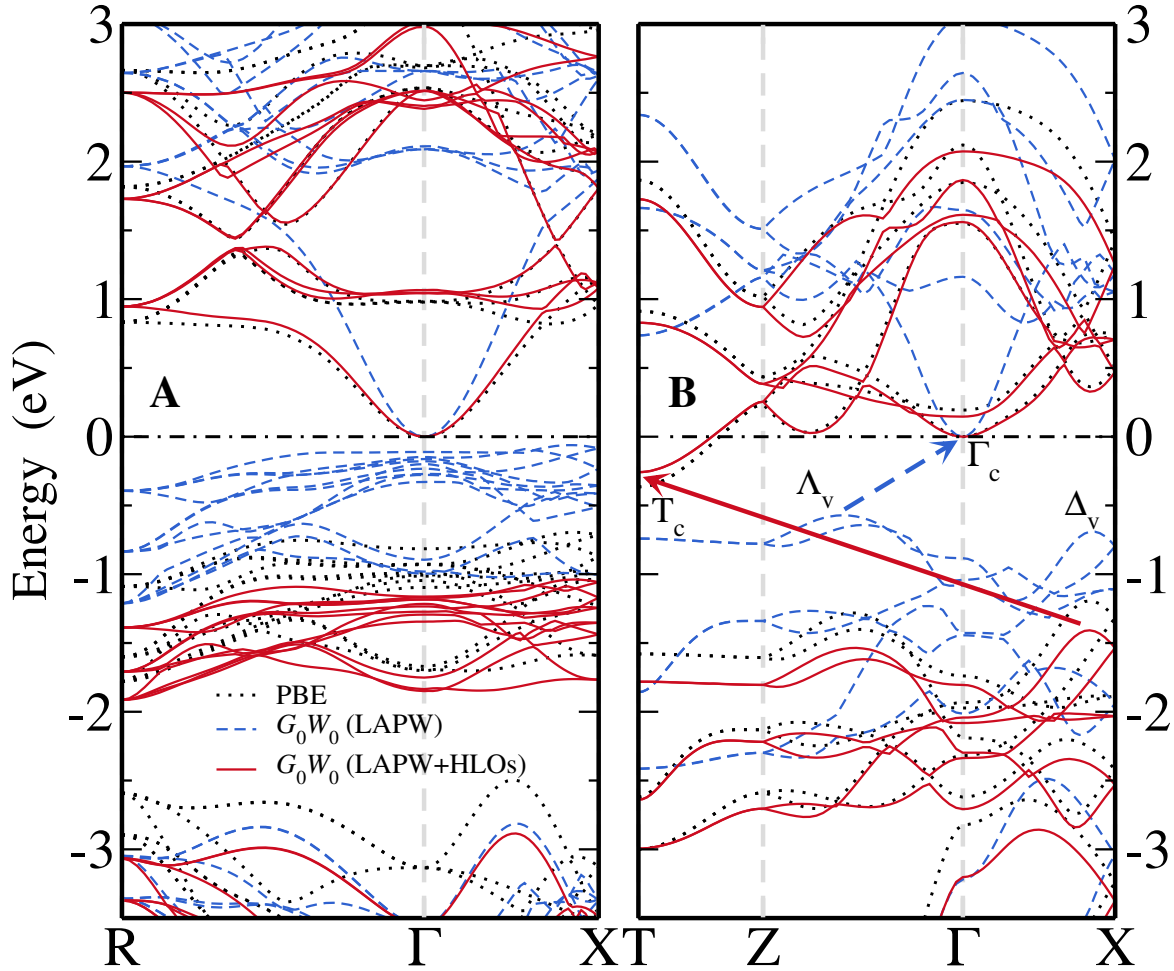

A: pyrite phase, B: marcasite phase

M.-Y. Zhang and H. Jiang, Front. Chem. **9**, 747972 (2021)

Summary

We talked about

- necessary ingredients to implement a G_0W_0 method on top of mean-field result
- examples that GW method works "simply" or with careful treatment

Recent advancements & outlook

- Apparatus designed for better converging QP band structure in low-dimensional systems [1]
- Elimination of unoccupied states in computing P and Σ^c [2]
- Techniques and library to enable low-scaling calculation [3]
- Improvement on analytic continuation or exact contour deformation to treat frequency dependence [4]
- Beyond-*GW*@ DFA approaches: vertex correction, GW+DMFT [5]

---

[1] F. H. da Jornada, D. Y. Qiu, and S. G. Louie, Phys. Rev. B **95**, 035109 (2017), F. Hüser, T. Olsen, and K. S. Thygesen, Phys. Rev. B **88**, 245309 (2013)

[2] M. Govoni and G. Galli, J. Chem. Theory Comput. **11**, 2680–2696 (2015), M. Govoni and G. Galli, J. Chem. Theory Comput. **14**, 1895–1909 (2018)

[3] P. Liu et al., Phys. Rev. B **94**, 165109 (2016), J. Wilhelm, P. Seewald, and D. Golze, J. Chem. Theory Comput. **17**, 1662–1677 (2021); GreenX library by NOMAD CoE WP2

[4] I. Duchemin and X. Blase, J. Chem. Theory Comput. **17**, 2383–2393 (2021), J. Fei, C.-N. Yeh, and E. Gull, Phys. Rev. Lett. **126**, 056402 (2021)

[5] H. Ma et al., J. Chem. Theory Comput. **15**, 154–164 (2019), T. Zhu and G. K.-L. Chan, Phys. Rev. X **11**, 021006 (2021)

Thank you for listening!

References I

[1] O. K. Andersen, Phys. Rev. B **12**, 3060–3083 (1975).

[2] F. Aryasetiawan and O. Gunnarsson, Phys. Rev. B **49**, 16214–16222 (1994).

[3] F. Aryasetiawan and O. Gunnarsson, Rep. Prog. Phys. **61**, 237 (1998).

[4] Z.-H. Cui et al., J. Phys. Chem. Lett. **9**, 2338–2345 (2018).

[5] F. H. da Jornada, D. Y. Qiu, and S. G. Louie, Phys. Rev. B **95**, 035109 (2017).

[6] I. Duchemin and X. Blase, J. Chem. Theory Comput. **17**, 2383–2393 (2021).

[7] E. Engel and R. M. Dreizler, *Density Functional Theory: An Advanced Course*, (Springer Science & Business Media, 2011), 543 pp.

[8] A. Ennaoui et al., Sol. Energy Mater. Sol. Cells **29**, 289–370 (1993).

[9] J. Fei, C.-N. Yeh, and E. Gull, Phys. Rev. Lett. **126**, 056402 (2021).

[10] D. Golze, M. Dvorak, and P. Rinke, Front. Chem. **7**, 377 (2019).

[11] M. Govoni and G. Galli, J. Chem. Theory Comput. **11**, 2680–2696 (2015).

[12] M. Govoni and G. Galli, J. Chem. Theory Comput. **14**, 1895–1909 (2018).

[13] G. Greczynski and L. Hultman, Prog. Mater Sci. **107**, 100591 (2020).

[14] F. Gygi and A. Baldereschi, Phys. Rev. B **34**, 4405–4408 (1986).

References II

[15] L. Hedin, Phys. Rev. **139**, A796–A823 (1965).

[16] F. Hüser, T. Olsen, and K. S. Thygesen, Phys. Rev. B **88**, 245309 (2013).

[17] M. S. Hybertsen and S. G. Louie, Phys. Rev. B **34**, 5390–5413 (1986).

[18] H. Jiang and P. Blaha, Phys. Rev. B **93**, 115203 (2016).

[19] H. Jiang et al., Comput. Phys. Commun. **184**, 348–366 (2013).

[20] J. Klimeš, M. Kaltak, and G. Kresse, Phys. Rev. B **90**, 075125 (2014).

[21] R. Laskowski and P. Blaha, Phys. Rev. B **85**, 035132 (2012).

[22] B. Liu et al., Adv. Mater. **28**, 6457–6464 (2016).

[23] P. Liu et al., Phys. Rev. B **94**, 165109 (2016).

[24] H. Ma et al., J. Chem. Theory Comput. **15**, 154–164 (2019).

[25] K. Maeda and K. Domen, J. Phys. Chem. C **111**, 7851–7861 (2007).

[26] S. Massidda, M. Posternak, and A. Baldereschi, Phys. Rev. B **48**, 5058–5068 (1993).

[27] B. R. A. Nijboer and F. W. De Wette, Physica **23**, 309–321 (1957).

[28] X. Ren et al., Phys. Rev. Materials **5**, 013807 (2021).

[29] H. N. Rojas, R. W. Godby, and R. J. Needs, Phys. Rev. Lett. **74**, 1827 (1995).

References III

[30] T. Schena, G. Bihlmayer, and S. Blügel, Phys. Rev. B **88**, 235203 (2013).

[31] M. van Schilfgaarde, T. Kotani, and S. Faleev, Phys. Rev. Lett. **96**, 226402 (2006).

[32] M. van Schilfgaarde, T. Kotani, and S. V. Faleev, Phys. Rev. B **74**, 245125 (2006).

[33] A. Seidl et al., Phys. Rev. B **53**, 3764–3774 (1996).

[34] M. Shishkin and G. Kresse, Phys. Rev. B **75**, 235102 (2007).

[35] D. Singh, Phys. Rev. B **43**, 6388–6392 (1991).

[36] J. C. Slater, Phys. Rev. **51**, 846–851 (1937).

[37] J. Tejeda et al., Phys. Rev. B **12**, 1557–1566 (1975).

[38] F. Tran, S. Ehsan, and P. Blaha, Phys. Rev. Materials **2**, 023802 (2018).

[39] M. Usuda et al., Phys. Rev. B **66**, 125101 (2002).

[40] T. J. Whittles et al., Chem. Mater. **28**, 3718–3726 (2016).

[41] J. Wilhelm, P. Seewald, and D. Golze, J. Chem. Theory Comput. **17**, 1662–1677 (2021).

[42] M.-Y. Zhang and H. Jiang, Front. Chem. **9**, 747972 (2021).

[43] T. Zhu and G. K.-L. Chan, Phys. Rev. X **11**, 021006 (2021).

Photoelectron (PE) spectroscopy

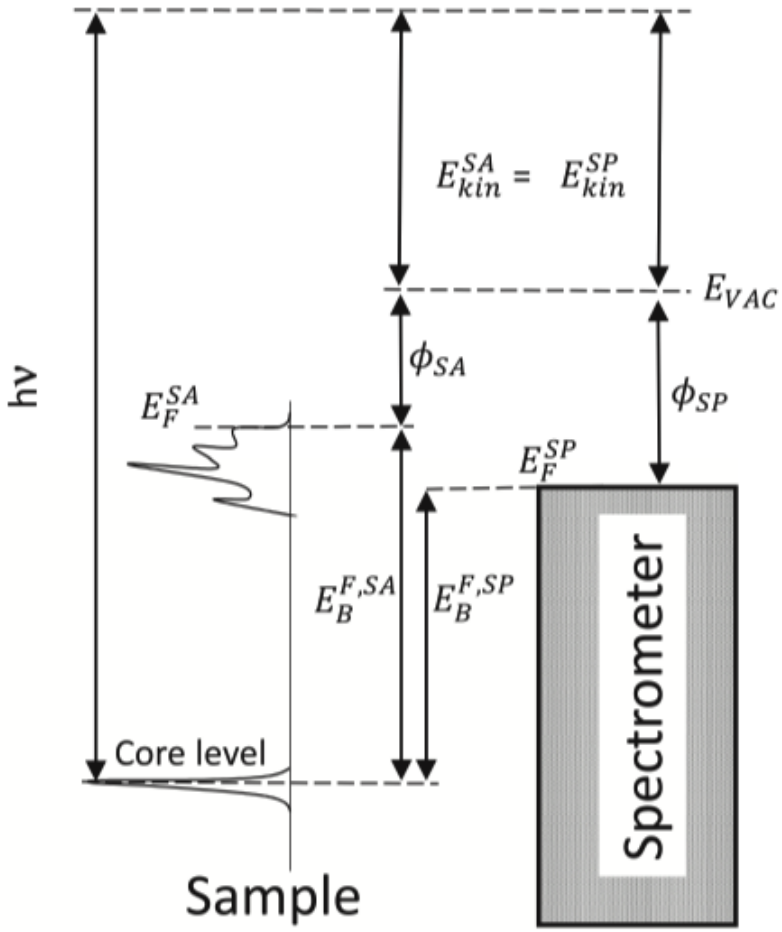

Binding energy

$$E_B^{ref} = -(E - E^{ref})$$

Using different references

$$\begin{aligned} h\nu &= E_B^{F,SA} + \phi_{SA} + E_{kin}^{SA} \\ &= E_B^{F,SP} + \phi_{SP} + E_{kin}^{SP} \\ \Rightarrow E_B^{F,SP} &= h\nu - E_{kin}^{SP} - \phi_{SP} \end{aligned}$$

ϕ_{SP} is a constant fixed by calibration.

Popular choices include

- UPS: Fermi level of noble metal
- XPS: (semi-)core level: Au $4f_{7/2}$, Ag $3d_{5/2}$

G. Greczynski and L. Hultman, Prog. Mater Sci. **107**, 100591 (2020)

Photoelectron (PE) spectroscopy

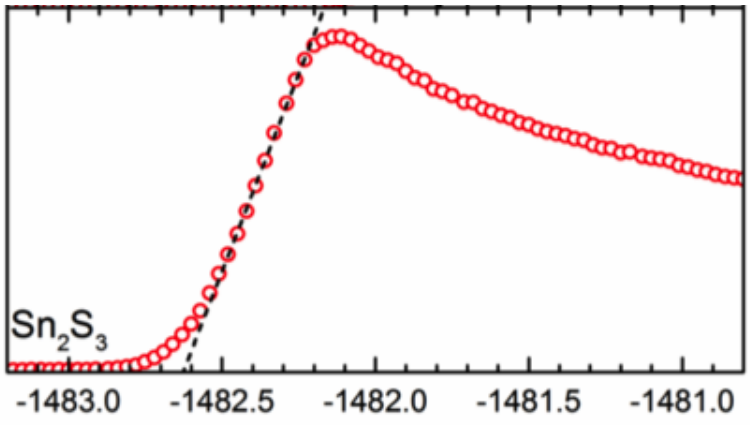

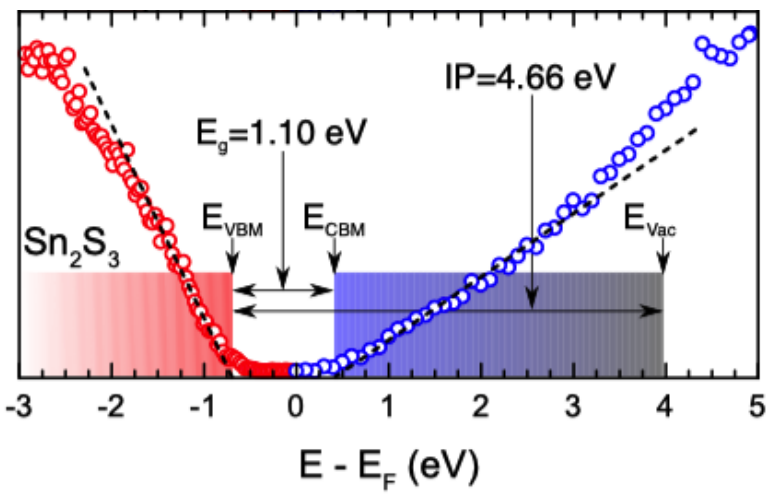

Al Kα: $h\nu = 1486.6$ eV

Second-electron cut-off corresponds to zero-KE PE, i.e. at vacuum level

$$h\nu - E^{F,SP}_{B,SEC} = E_{vac}$$

Absolute energy of top valence band

$$\phi_{SA} - E^{F,SP}_{B,V} = E_{vac}$$

$$\Rightarrow \phi_{SA} = h\nu - E^{F,SP}_{B,SEC} + E^{F,SP}_{B,V}$$

In case of Sn_2S_3

$$\phi \approx 1486.6 - 1482.6 + 0.7 = 4.7 \text{ eV}$$

(Ag reference 4.4 ± 0.3 eV)

J. Tejeda et al., Phys. Rev. B **12**, 1557–1566 (1975), T. J. Whittles et al., Chem. Mater. **28**, 3718–3726 (2016)

Optical absorption and photoluminescence

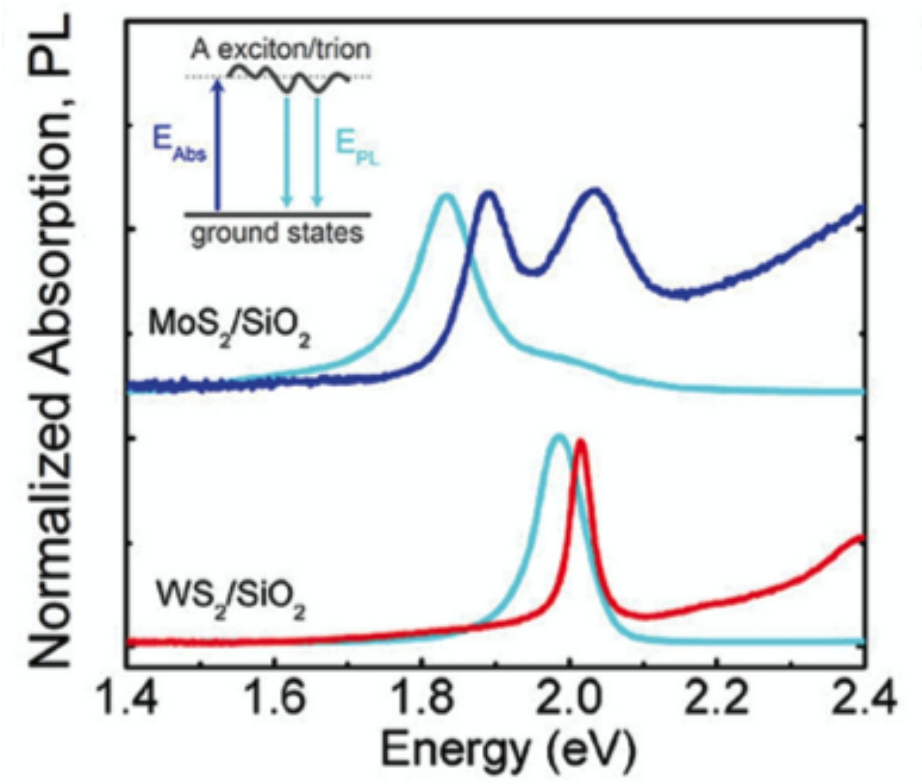

Excitonic feature of ml-$\{Mo, W\}S_2$

- doublet in absorption, due to SOC in valence states at K
- Stokes shift $\sim 10^1$ meV, depending on doping/substrate

B. Liu et al., Adv. Mater. **28**, 6457–6464 (2016)

Local orbitals (LOs) in LAPW framework

$$\varphi^{\mathrm{LO}}_{alm,p}(\mathbf{r}) = \begin{cases} \left[\begin{array}{c} A_{alm,p} u_{al}(r^a; E_{al}) + \\ B_{alm,p} \dot{u}_{al}(r^a; E_{al}) + C_{alm,p} u_{al}(r^a; E^p_{al}) \end{array} \right] Y_{lm}(\hat{\mathbf{r}}^a) & \mathbf{r} \in V^a \\ 0 & \mathbf{r} \in I \end{cases}$$

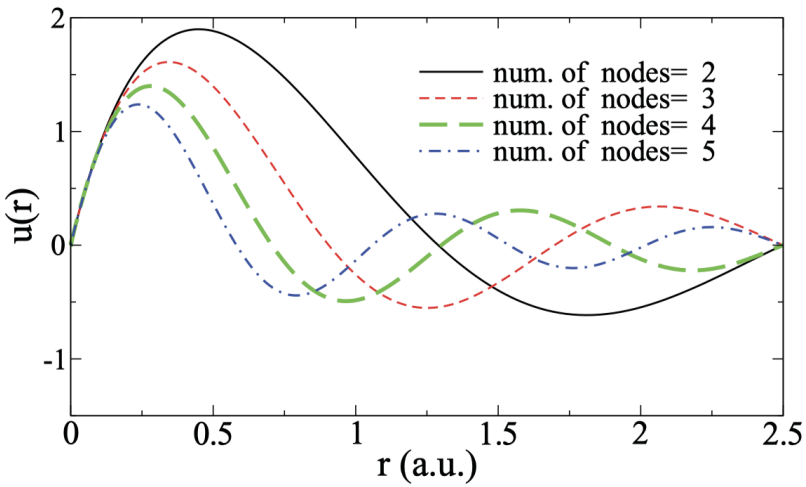

High-energy LOs: LOs having large E^p_{al} with increasing node numbers

R. Laskowski and P. Blaha, Phys. Rev. B **85**, 035132 (2012), D. Singh, Phys. Rev. B **43**, 6388–6392 (1991)

Augmented plane-wave basis

Originally proposed by Slater: divide the cell into spheres around atomic nuclei a (called muffin-tin, MT) and interstitial region

$$\varphi_{\mathbf{kG}}^{\mathrm{APW}}(\mathbf{r}) = \begin{cases} \sum_{lm} A_{alm}(\mathbf{k}+\mathbf{G}) u_{al}(r^a; E) Y_{lm}(\hat{\mathbf{r}}^a) & \mathbf{r} \in V^a \\ \frac{1}{\sqrt{V}} \mathrm{e}^{\mathrm{i}(\mathbf{k}+\mathbf{G})\cdot\mathbf{r}} & \mathbf{r} \in I \end{cases}$$

To avoid solving a transcedental equation, the radial function is linearized at some reference energy

$$\varphi_{\mathbf{kG}}^{\mathrm{LAPW}}(\mathbf{r}) = \begin{cases} \sum_{lm} \begin{bmatrix} A_{alm}(\mathbf{k}+\mathbf{G}) u_{al}(r^a; E_{al}) \\ +B_{alm}(\mathbf{k}+\mathbf{G}) \dot{u}_{al}(r^a; E_{al}) \end{bmatrix} Y_{lm}(\hat{\mathbf{r}}^a) & \mathbf{r} \in V^a \\ \frac{1}{\sqrt{V}} \mathrm{e}^{\mathrm{i}(\mathbf{k}+\mathbf{G})\cdot\mathbf{r}} & \mathbf{r} \in I \end{cases}$$

For semi-core states like 3d, local orbital inside MT at similar energy is typyically included.

J. C. Slater, Phys. Rev. **51**, 846–851 (1937)
O. K. Andersen, Phys. Rev. B **12**, 3060–3083 (1975)